Hot gas desulphurisation with dolomite sorbent in coal gasification

Ramón Álvarez-Rodríguez *, Carmen Clemente-Jul

Mining School, Technical University of Madrid (UPM), C/Rios Rosas, 21, 28003 Madrid, Spain

Keywords:
Gasification
Desulphurisation
Dolomite
Coal

A B S T R A C T

Gasification technologies are among the most promising electrical power generation options both from an environmental and efficiency point of view, as they allow efficient, environmentally-friendly use of national coal, as well as other carbonaceous materials mixed with coal, including high sulphur by-products.

During gasification, sulphur is converted mainly into H_2S and secondly into COS, and control of these has been researched using several H_2S adsorbents. The aim of this paper was advanced removal of these compounds.

Dolomite, which reacts with H_2S to yield calcium sulphide, was chosen from among several earth-alkaline compounds for research due to its properties and low cost in reducing the presence of H_2S in coal gasification.

Tests were carried out using dolomite from Granada, Spain, with this sorbent used without blending and with amounts of 100 g and 150 g in each test. The dolomite was sulphurized using a mixture of gases that simulates the gasification gas.

The influence of sulphurisation conditions such as gas velocity, bed length, grain size, gas temperature, and gas composition were investigated. The solid products obtained were characterised by X-ray diffraction and chemical analysis.

The behaviour of COS that normally accompanies H_2S in gasification gases was investigated and found to follow a breakthrough curve similar to H_2S, with equilibrium existing between the COS destroyed due to reaction with hydrogen and by hydrolysis and the COS formed by reaction of CO_2 with H_2S. Hence, its content in outlet gases is a function of the composition of this gas, especially in terms of CO_2, H_2S and H_2O.

The accelerating effect of sulphurised dolomite on the rate of the reverse water-shift reaction was demonstrated.

1. Introduction

In the gasification of coal or blends with other alternative fuels, sulphur is mainly present in the gas as hydrogen sulphide. This sulphur compound must be removed prior to gas combustion to comply with legislation and especially to avoid damage to the turbines. In the chemical industry, the presence of H_2S leads to larger corrosion problems (pipes, compressors, etc.) and also problems with some catalysts. The scrubbing of sulphur from the gas stream has been widely studied using different agents, such as the amines used by Elcogas IGCC in Spain; however, this option requires a decrease in gas temperature that causes the inherent energy losses.

Some sorbents that allow H_2S to be removed at high temperatures have been previously investigated; these include diverse metal compounds Sorbent regeneration without significant degradation during a certain number of cycles is extremely important. Several Zn compounds some Mn and Cu compounds and blends and some Fe compounds have also been studied. The main problem is the sufficient duration of cycles without degradation. One very cheap oxide, CaO, that does not need to be reused has also been studied. The main sources are two abundant minerals, calcite and dolomite. The direct addition of this oxide or the calcite in the gasification bed for coal gasification or the gasification of other alternative fuels has been investigated not only to clean the gas, but to produce hydrogen and also the absorption of H_2S in the oxides to remove them from the gas

Calcium oxide is effective in adsorbing H_2S from the gasification gases according to the reaction:

$$H_2S + CaO \leftrightarrow CaS + H_2O_{(g)} \quad \Delta H^0 = -59.2 \text{ kJ mol}^{-1} \tag{1}$$

but many studies with calcite or dolomite have been carried out on small samples in a thermobalance or differential reactor with 1 mg to 1 g In other cases, larger amounts of absorbent have been used but mixed with silica grains to form a homogeneous

mixture of sorbent and silica to avoid improper random distribution of the gas flow and reduce errors in the longitudinal conversion of profiles as in articles with the aim of obtaining appropriate measures to develop mathematical models.

In the case of an industrial application it would be appropriate to apply the pure absorbent which is why this investigation was carried out in this way and the different behaviour investigated according to grain size and position in the absorbent column: at the top or at the bottom subjected to more mechanical pressure. Absorbent amounts of 100 g and 150 g that give bed lengths of 11.4 and 17 cm, respectively, were also used.

The absorbent chosen was dolomite as it works well under calcining (1123 K) and non-calcining conditions (1173 K) according to previous studied by Adanez

H_2S in the gasification gases is known to be accompanied by a certain proportion of carbonyl sulphide (COS) that when burnt, yields SO_2 according to the following reaction:

$$COS + 3/2O_2 \leftrightarrow CO_2 + SO_2 \quad \Delta H^0 = -552 \text{ kJ mol}^{-1} \tag{2}$$

This reaction increases the SO_2 content of gases and increases the corrosive effect in gas turbines, gas motors, pipes and general industrial equipment and also increases SO_2 emissions. Therefore, it should be reduced. At Elcogas, for example, this is carried out by COS hydrolysis according to the following reaction

$$COS + H_2O_{(g)} \leftrightarrow H_2S + CO_2 \quad \Delta H^0 = -33.6 \text{ kJ mol}^{-1} \tag{3}$$

H_2S is later eliminated by amine extraction.

There are various studies on COS hydrolysis especially aimed at the development of new catalysts such as rare earth oxysulphides , but that require operating at relatively low temperatures.

However, the ability to reduce COS at high temperatures using the same approach as H_2S on earth alkaline sorbents would be of interest. This possibility has already been studied by Heesink but limited to lower temperature (up to 700 °C) and with a very small amount of sorbent and that postulates the reaction:

$$CaO + COS \leftrightarrow CaS + CO_2 \quad \Delta H^0 = -90 \text{ kJ mol}^{-1} \tag{4}$$

Ishida also postulates the reactions:

$$CO_2 + H_2S \leftrightarrow COS + H_2O_{(g)} \quad \Delta H^0 = +33.6 \text{ kJ mol}^{-1} \tag{5}$$

$$CO_2 + 2H_2S \leftrightarrow CS_2 + 2H_2O_{(g)} \quad \Delta H^0 = +68 \text{ kJ mol}^{-1} \tag{6}$$

The proportion of COS to be expected will also depend on the concentrations of CO_2, H_2S and H_2O (reaction (5) is the reverse of (3)).

To achieve a reduction in H_2S and COS levels at very low values, some authors use Zn composites as absorbents that carry out desulphurisation over two stages, one to reduce the high level of H_2S at a low value, followed by another stage that uses an especially prepared absorbent with a high specific surface area.

In the present study, H_2S was contaminated with a small amount of COS (about 1% of the H_2S content) with the aim of investigating any decreases or increases under the test conditions, now operating with relatively large amounts of 100 g or 150 g of material. The contamination is sufficiently low so as not to decisively influence the principal sulphidisation reaction with hydrogen sulphide (1).

Another important reaction to consider is the reverse water-shift reaction, which influences the proportion of H_2 in the outlet gases, an important aspect if hydrogen is to be produced:

$$CO_2 + H_2 \leftrightarrow CO + H_2O \quad \Delta H^0 = +41.1 \text{ kJ mol}^{-1} \tag{7}$$

2. Experimental

All experiments were performed using a dolomite from the province of Granada, Spain, that presented an essentially theoretical composition. The X-ray diffractogram and analysis are shown in Fig. 1 and Table 1, respectively. The chemical analysis was performed by X-ray fluorescence for the aforementioned elements and by gravimetric methods for insoluble material and loss on ignition.

This dolomite can be completely decomposed at 850 °C as shown in Fig. 2, which contains the thermogram for dolomite in a nitrogen atmosphere (40 cm^3/min) with a temperature increase of 10 °C/min up to 850 °C, followed by constant temperature. A Setaram-Labsys thermobalance was used to obtain the thermograms.

The tests were conducted with a Kanthal vertical tubular reactor with a length of 1.6 m and inner diameter of 27 mm, which passes, in its central part, through a furnace with an inner length of 600 mm. This equipment was practically identical to the one used by Adánez (see Fig. 3).

The desulphuring column, laid out as a fixed bed, was formed by using 100 g or 150 g of dolomite classified granulometrically at 0.4–0.5 mm, 0.71–1 mm and 2–2.5 mm to obtain the different behaviour according to grain size. The dolomite was left at the top of the desulphuring column to study this relative position or at the bottom of a column of 250 g of silica of 1.6–2 mm (yielding a bed length of 30 cm) to study the behaviour of absorbent located toward the bottom of a desulphuring bed under more static pressure (Fig. 3).

The initial sulphidising gases were introduced through the upper part of the reactor in order to flow across the bed of material to be sulphidised. These gases then came out through the lower end and flow through a coolant to separate out the water before the gases are analysed in a Varian CP-4900 Micro-GC gas analyser equipped with a 10 m column of Porabond Q and a thermal conductivity detector that took a sample every 5.7–6 min. The gases are analysed for H_2S, COS, SO_2 and CO_2.

To carry out sulphidisation tests, the dolomite sample was initially heated at 850 °C, 900 °C or 950 °C (temperature measured by a thermocouple in contact with the dolomite sample) in a nitrogen atmosphere of 10 l/min, which caused it to decompose. The time necessary to detect a CO_2 content of less of 100 ppm was noted and then the temperature was stabilised with the gas mixture at the velocity to be used, except H_2S and H_2 and balanced with N_2. The furnace resistor temperature was adjusted, as appropriate, to stabilise the temperature at the desired value.

Sulphidisation was produced by injecting the H_2S and H_2 mixture and reducing N_2 by the same amount. Gases continued to be added at 12.5, 10 and 5 l/min (36.4, 29.1 and 14.5 cm s^{-1}), considered by several authors as a typical case of plug flow . All gases were monitored by specific mass flow controllers and steam was obtained by complete evaporation of constant water flow moni-

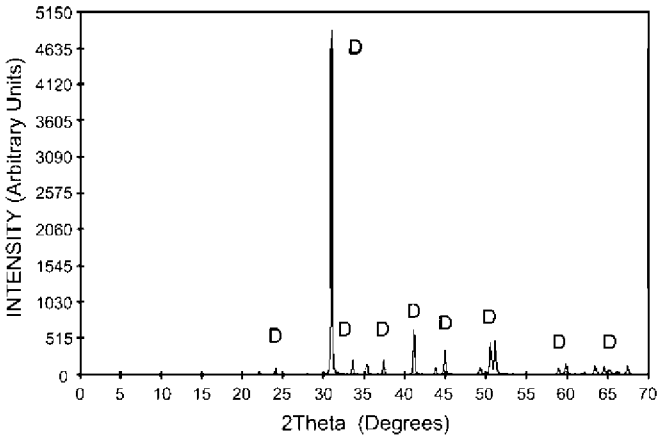

Fig. 1. Diffractogram of Granada dolomite used (D: dolomite).

Table 1
Granada dolomite analysis

Element	Content%
CaO	30.51
MgO	21.68
Fe_2O_3	0.06
MnO	0.007
TiO_2	0.006
SiO_2	0.1
Al_2O_3	<0.1
K_2O	<0.1
Na_2O	<0.1
P_2O_5	<0.05
Insoluble	0.20
Loss on ignition	47.53

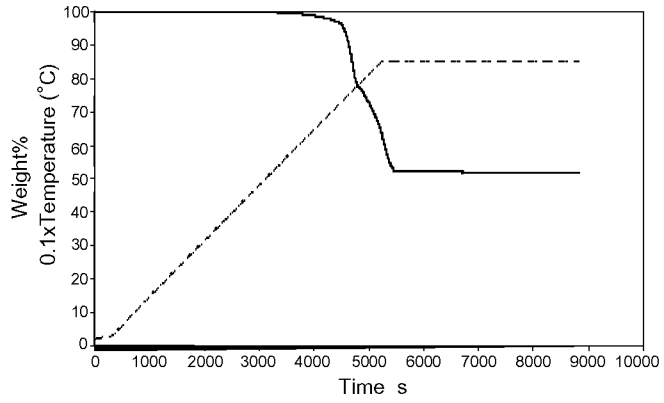

Fig. 2. Thermogram of the dolomite used (– weight, -- temperature).

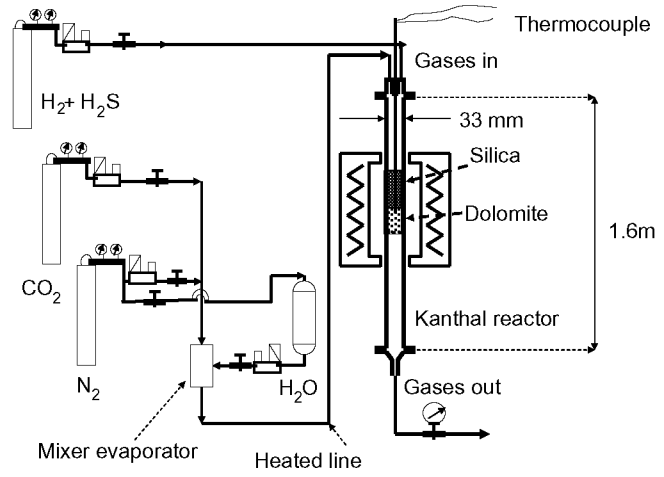

Fig. 3. Simplified chart of the system used. Dolomite at bottom position below a silica column.

tored by a mass flow controller and evaporator mixer. The certified deviations of the mass flow controllers (for flows measured under 75% of the fond scale) were lower than ±0.3% of FS (±0.03 l/min for N_2 and 0.009 l/min for other gases).

Once the concentration of H_2S coming out was stabilised and approximately the same as the one being injected (except for changes in the minute amount of COS), sulphidisation is completed. First, all gases were cut off except N_2 and $H_2S + H_2$ and after a short time, H_2S was also cut off and then a N_2 stream was passed to eliminate any gases that could impregnate the sample whilst the reactor was cooled by stopping the furnace current and opening the furnace.

The sulphidised sample was collected and analysed by X-ray diffraction and by chemical analysis when changing the sample size to control the degree of sulphidisation. All chemical analyses were done using gravimetric methods. A Phillips PX-1710 X-ray diffractometer was used.

Sulphidisation gases were formed from a mixture of gases: pure N_2 as balance gas, pure CO_2, pure steam, and a certified commercial mixture of 10% H_2S and 90% H_2 (H_2S relative uncertainty of 2%), that contains about 0.1% COS monitored by gas chromatography according to certified standards, to obtain a sulphurisation gas with approximately 2% H_2S to simulate gasification of sulphur-rich materials such as pet-coke, some coals, etc. and with another certified commercial mix of 2% H_2S and 98% H_2 (H_2S relative uncertainty of 2%) with approximately 0.02% COS to obtain a gas for sulphurisation with 0.4% of H_2S and 19.6% of H_2 to simulate the gasification of sulphur-poor substances.

The tests were carried out at atmospheric pressure with a slight excess pressure of approximately 0.1 bar to simulate the necessary pressure to circulate the gas; the pressure was 0.11 MPa.

Because hydrogen production is and will be important in the future and the shift reaction can be used for this and because gases to be desulphured do not have to be in equilibrium at the sulphidisation temperatures studied (850–950 °C), it was decided to study the behaviour of reaction (7) by not introducing CO, but rather by forming CO via a reaction between the CO_2 introduced and the hydrogen existing in the mixture. The action of the dolomite was then compared to the action of the silica (inert material).

The conditions used to test the dolomite are shown in Table 2, along with other duplicate tests to confirm the results.

Tests were also carried out by replacing dolomite with silica, especially to study the behaviour of COS and the reverse water-shift reaction (Table 2).

3. Results and discussion

3.1. Absorption of hydrogen sulphide

3.1.1. Influence of grain size, gas velocity and relative position in the desulphuring column (top or bottom)

By operating as described in Section 2, virtually complete (98–99%) dolomite sulphidisation is obtained when the higher grain size of 2–2.5 mm was used, which would be the most difficult to sulphurise under different test conditions. Fig. 4 shows the X-ray diffraction of sulphurised dolomite, which contains no line of $CaSO_4$ or CaO, but rather only CaS (oldhamite) and MgO (periclase) lines.

Fig. 5 shows the breakthrough curves from various tests carried out at a gas velocity of 29.1 and 14.5 cm s^{-1} and considering the case of dolomite at the bottom of the desulphuring column under more static pressure (tests 2,3,7,9,10 and 11; Table 2) and a test carried out with dolomite at the top of the column (test 6).

The H_2S concentration of the outlet gas has been plotted as a percentage with respect to the maximum output: 100% corresponds to approximately 20,000 ppm of H_2S, but not exactly as there are small variations due to a small variation in the proportions of outlet COS (see Section 3.2).

To explain the influence of the gas velocity, it was observed that the curves (for the three grain sizes) carried out at lower velocity are shifted toward the right but approximately retained their shape, a finding that is consistent with previous studies [19]. This occurs because a lower gas velocity was used, which meant that the amount of H_2S introduced per time unit was lower and that more time was needed to reach a definite degree of saturation.

Table 2
Test Conditions for Calcined Dolomite Sulphurisation

Test conditions							Inlet gas (N_2 balance gas)				
Test	Material	Grain size (mm)	Temp (K)	Bed length (cm)	Gas velocity (cm s^{-1})	Dolomite position (top or bottom)	H_2S%	COS (ppm)	H_2%	CO_2%	H_2O%
1	Dolomite	0.4–0.5	1123	11.4	29.1	T	2	176	18	6	10
2	Dolomite	0.4–0.5	1123	11.4	29.1	B	2	176	18	6	10
3	Dolomite	0.4–0.5	1123	11.4	14.5	B	2	176	18	6	10
4	Dolomite	0.71–1	1123	11.4	36.4	T	2	176	18	6	10
5	Dolomite	0.71–1	1123	11.4	36.4	T	2	176	18	–	–
6	Dolomite	0.71–1	1123	11.4	29.1	T	2	176	18	6	10
7	Dolomite	0.71–1	1123	11.4	29.1	B	2	176	18	–	–
8	Dolomite	0.71–1	1123	17	29.1	T	2	176	18	–	10
9	Dolomite	0.71–1	1123	11.4	14.5	B	2	176	18	6	10
10	Dolomite	2–2.5	1123	11.4	29.1	B	2	176	18	6	10
11	Dolomite	2–2.5	1123	11.4	14.5	B	2	176	18	6	10
12	Dolomite	2–2.5	1123	17	14.5	B	2	176	18	6	10
13	Dolomite	2–2.5	1173	11.4	14.5	B	2	176	18	6	10
14	Dolomite	2–2.5	1173	17	14.5	B	2	176	18	6	10
15	Dolomite	2–2.5	1223	11.4	14.5	B	2	176	18	6	10
16	Dolomite	2–2.5	1123	11.4	14.5	B	2	176	18	6	–
17	Dolomite	2–2.5	1123	11.4	29.1	B	0.4	38	19.6	6	10
18	Dolomite	2–2.5	1123	17	14.5	B	0.4	38	19.6	6	10
19	Silica	1.6–2	1123	11.4	14.5	B	2	176	18	–	–
20	Silica	1.6–2	1123	11.4	14.5	B	2	176	18	6	10
21	Silica	1.6–2	1123	11.4	14.5	B	0.4	38	19.6	–	–
22	Silica	1.6–2	1123	11.4	14.5	B	0.4	38	19.6	6	10
23	Silica	1.6–2	1123	11.4	14.5	B	0.4	38	19.6	6	–

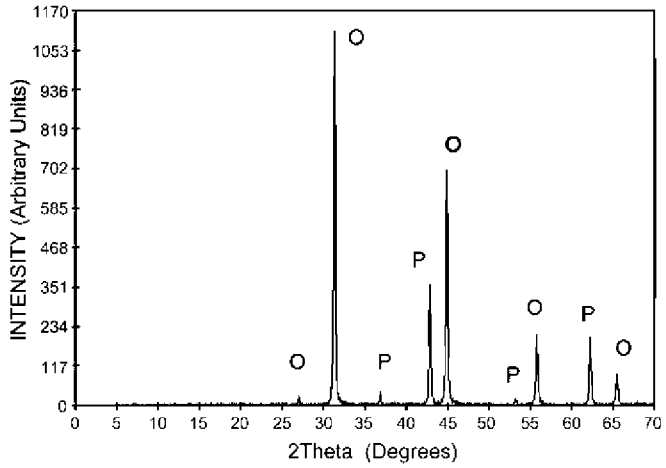

Fig. 4. Diffractogram of sulphurised Granada dolomite (O: oldhamite, P: periclase).

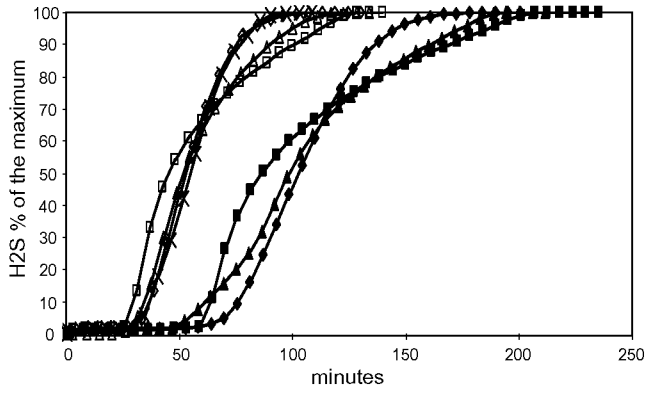

Fig. 5. Influence of grain size, gas velocity and relative position. Breakthrough curves for 11.4-cm bed length (Table 2): with dolomite at top position, test 6 (×, 0.71 mm, 29.1 cm s^{-1} gas velocity). With dolomite at bottom position and with 29.1 cm s^{-1} g.v., tests 2 (□, 0.4 mm), 7 (Δ, 0.71 mm), 10 (◇, 2 mm), and with 14.5 cm s^{-1} g.v., tests 3 (■, 0.4 mm), 9 (▲, 0.71 mm) and 11(♦, 2 mm)

To explain the influence of grain size, it was observed that the curves corresponding to lower granulometries (0.4–0.5 mm) at the bottom have a flatter gradient than those corresponding to 2–2.5 mm at both gas velocities of 29.1 and 14.5 cm s^{-1}. The tests with a grain size of 0.71 have an intermediate position. This shows that lower grain sizes results in greater grain packing in a compact bed of dolomite grains, thus creating preferential paths for the gas and delaying H_2S absorption. Therefore, under the conditions used, this means that a grain size of 2–2.5 mm will yield better results.

The effect of dolomite position can be observed by comparing the grain size of 0.71 mm with breakthrough curves at 29.1 cm s^{-1}, one at the top and the other at the bottom. At the bottom position, the gradient is flatter.

The 0.71 mm curve at top position can also be compared with the curve of 2–2.5 mm at the bottom position, both at 29.1 cm s^{-1}: the curves are practically identical and have the shape of the breakthrough curves obtained by Adánez et al. (especially the curve for 0.71 mm) who used silica mixtures to obtain more uniform permeability and to adjust the mathematical models. Under the conditions used, the curves at the bottom with the shape most closely resembling the mathematical models are those corresponding to a larger grain size (2–2.5 mm), in contrast with [19].

3.1.2. Influence of temperature (850 °C, 900 °C or 950 °C)

Fig. 5 shows three curves for 100 g of sample (11.4 cm bed thickness) and 2–2.5 grain size, in bottom position sulphuring with 14.5 cm s^{-1} gas velocity, 2% H_2S and temperatures of 1123 K, 1173 K and 1223 K (test 11, 13, and 15, Table 2).

Almost no differences in curve shape and values were observed between sulphidisation temperatures of 1123 K, 1173 K and 1223 K, except for a difference in the smallest values (when a large part of the reagent had still has not reacted). This is consistent with other studies, but differs from the results obtained with calcite which showed a major variation in behaviour between 850 °C and 900 °C.

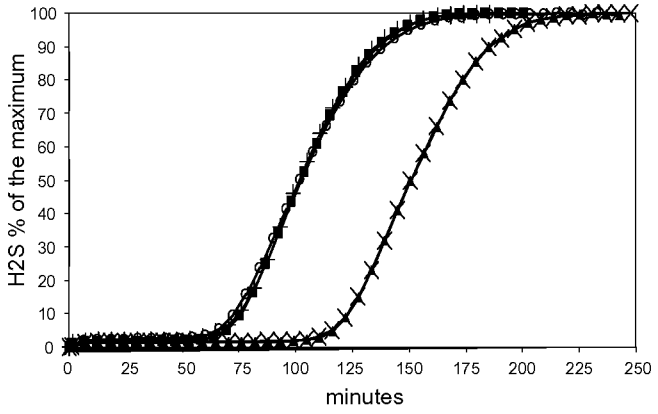

Fig. 6. Influence of temperature. Breakthrough curves at 850 °C for tests (Table 2) 11 (■, 11.4 cm) and 12 (▲, 17 cm). At 900 °C, tests 13 (+, 11.4 cm) and 14 (×, 17 cm). At 950 °C, test 15 (○, 11.4 cm).

The curves are essentially identical for the three temperatures and show little influence of temperature in the case of dolomite in general. The initial area of the curves, where H_2S is more absorbed, is the most interesting part to consider in a possible reduction of the content in this substance in industrial gasification gases. Fig. 7 shows this extended area and reveals how the curves continue to be similar, but those for 850 °C are a little below those for 900 °C and 950 °C. Therefore, a temperature of 850 °C should be used instead of 900 °C or 950 °C to minimise the amount of H_2S in the purified gas.

Figs. 6 and 7 also show two curves for 150 g (17 cm bed thickness) in bottom-position sulphuring with 14.5 cm s^{-1} gas velocity, 2% H_2S and temperatures of 1123 K, and 1173 K (tests 12 and 14, Table 2). Their behaviour under these results is similar to the previous curves.

The principal sulphurisation reaction is (1) and the value of its equilibrium constant for the case of calcining conditions can be expressed as

$$K = P_{H_2O}/P_{H_2S} = 1.13\exp(7262/T). \quad (8)$$

At the beginning of sulphidisation, when practically all H_2S is adsorbed and taking in account the water generated by this adsorption reaction (1) and the water generated by the reverse shift reaction (7), the H_2S values in equilibrium at 1123 K, 1173 K and 1223 K are 208, 278 and 361 ppm, respectively (when 2% H_2S, 18% H_2, 6% CO_2 and 10% H_2O balanced with nitrogen are used). The higher the temperature, the higher the values of the H_2S concentration in equilibrium in accordance with the results presented.

These theoretical values are lower than the values observed for each set of parameters. Fig. 7 shows a plot of the theoretical value at 850 °C which clearly indicates the difference.

3.1.3. Influence of bed length

Figs. 6 and 7 also show this influence in some tests with a grain size of only 2–2.5 mm. In Fig. 6 the breakthrough curves of the test using 11.4 cm of bed length are grouped on the left side and those corresponding at 17 cm bed length are grouped on the right. There is a shift toward the right when bed length increases; this shift is independent of test temperature and occurs because a longer bed length means there is more solid to react and more time is needed to reach a particular conversion grade.

Fig. 7 contains a plot of the theoretical value of H_2S in equilibrium at 850 °C; this value is lower than the values observed at 850 °C (tests 11 and 12). The difference is greater in the case of 11.4 cm compared with 17 cm because there is more solid to react and more contact time between the gas and solid when 17 cm is used instead of 11.4 cm. This allows closer approximation to the theoretical value. Another conclusion is that even at the lower gas velocity used (14.5 cm s^{-1}), a 17-cm bed length is not enough to reach the theoretical value. Bed length is therefore an important parameter to narrow the gap between the potential results of a hypothetical industrial application and the theoretical values.

Fig. 8 also shows the influence of using a bed length of 11.4 or 17 cm under other conditions (tests 6, 8, 12 and 13; Table 2). Tests 12 and 13 (2.5-mm grain size, 14.5 cm s^{-1}) have been discussed previously and test 6 and 8 have the same grain size (0.71 mm), gas velocity (29.1), position (top) and temperature (850 °C). In test 8 (17 cm), the curve is shifted toward the right hand when compared to test 6 (11.4 cm bed length) and both curves have a similar gradient. Thus, this shift due to the bed length is produced with different grain sizes, gas velocities, sample positions in the desulphurising column, and temperatures.

Fig. 9 shows the initial part of the curves extended. The H_2S content of the outlet gases is lower with a longer bed length when compared with tests under other similar conditions, but with a shorter bed length.

3.1.4. Influence of H_2S concentration in initial gases

Fig. 10 shows an extension of the initial area of the breakthrough curves for several tests that jointly show tests performed

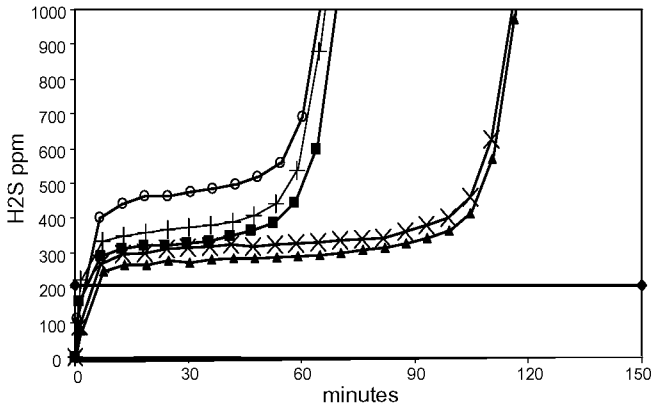

Fig. 7. Influence of temperature. Initial part of the breakthrough curves at 850 °C for tests (Table 2) 11 (■, 11.4 cm) and 12 (▲, 17 cm). At 900 °C, tests 13 (+, 11.4 cm) and 14 (×, 17 cm). At 950 °C, test 15 (○, 11.4 cm. Theoretical equilibrium 850 °C: horizontal line (♦).

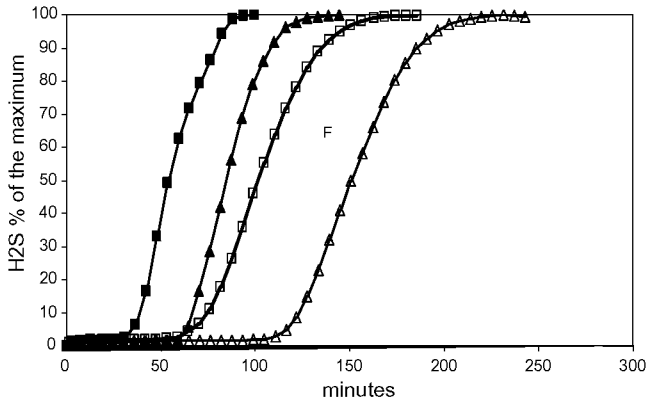

Fig. 8. Influence of bed length. Breakthrough curves for 11.4-cm: tests (Table 2) 6 (■, 0.71 mm, top position, 29.1 cm s^{-1} g.v.) and 13 (□, 2 mm, bottom position, 14.5 cm s^{-1} g.v.). For 17-cm, tests 8 (▲, 0.71 mm, top position, 29.1 cm s^{-1} g.v.) and 12 (Δ, 2 mm, bottom position, 14.5 cm s^{-1} g.v.).

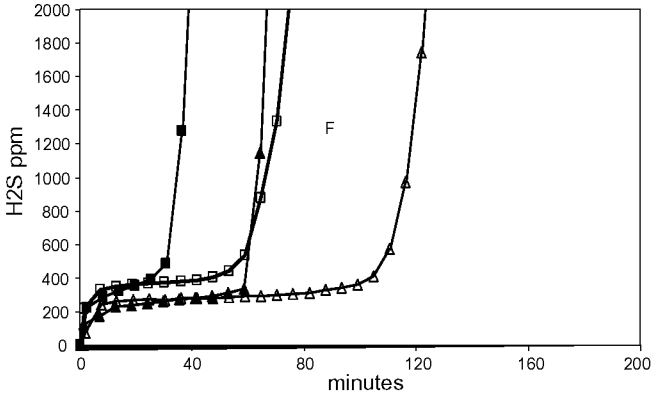

Fig. 9. Influence of bed length. Initial part of breakthrough curves for 11.4-cm: tests (Table 2) 6 (■, 0.71 mm, top position, 29.1 cm s^{-1} g.v.) and 13 (□, 2 mm, bottom position, 14.5 cm s^{-1} g.v.). For 17-cm, tests 8 (▲, 0.71 mm, top position, 29.1 cm s^{-1} g.v.) and 12 (Δ, 2 mm, bottom position, 14.5 cm s^{-1} g.v.).

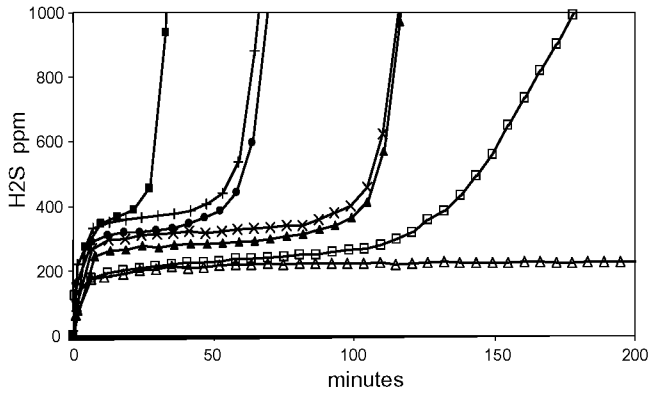

Fig. 10. Influence of H_2S concentration (2–2.5 mm grain size, bottom position). Initial part of breakthrough curves for 2% H_2S concentration, tests (Table 2) 10 (■,11.4 cm, 850 °C, 29.1 cm s^{-1} g.v.), 11 (●, 11.4 cm, 850 °C, 14.5 cm s^{-1} g.v.), 12 (▲, 17 cm, 850 °C, 14.5 cm s^{-1} g.v.), 13 (+, 11.4 cm, 900 °C, 14.5 cm s^{-1} g.v.),14 (×, 17 cm, 900 °C, 14.5 cm s^{-1} g.v.), and for 0.4% H_2S concentration, tests 17 (□, 11.4 cm, 850 °C, 29.1 cm s^{-1} g.v.) and 18 (Δ, 17 cm, 850 °C, 14.5 cm s^{-1} g.v.).

with 2% H_2S (tests 10,11,12,13,14) and tests with 0.4% H_2S (tests 17 and 18). Test 17 has the same operating parameters as test 10 except for H_2S concentration and test 18 has the same operating parameters as test 12 except for H_2S concentration. Tests 17 and 18 performed with a concentration of 0.4% H_2S have curves below the others. The decrease in the H_2S concentration of the inlet gases produces lower saturation at each point of the desulphurant column because there is less H_2S to react at any instant and relatively more free active points at any instant than at a higher H_2S concentration and therefore the reaction can produce results approaching the theoretical values.

The curves for tests 17 and 18 have a nearly flat initial stage that is practically identical; however, test 18 is slightly below test 17 due to longer bed length and lower velocity (Δ: 17 cm, 14.5 cm/s, instead of □: 11.4 cm, 29.1 cm s^{-1}).

3.1.5. Influence of composition of gas to be desulphured

Given the principal sulphurisation reaction (1), the presence of steam will obviously be one of the factors controlling the balance of the reaction.

In gasification gases, the presence of steam is normally 10% or higher and the presence of CO_2 may be around 3% in the case of entrained flow or higher in other cases. During sulphidisation, reaction (1) also yields water, especially in the initial stages in which nearly all H_2S reacts, which modifies the equilibrium.

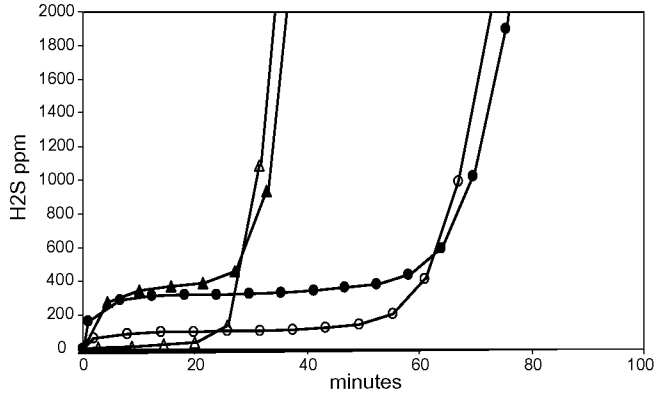

Fig. 11. Influence of gas composition (11.4 cm, 850 °C). Initial part of breakthrough curves with CO_2 and H_2O, tests (Table 2) 10 (▲, 29.1 cm s^{-1} g.v.) and 11 (●, 14.5 cm s^{-1} g.v.). With CO_2 and without H_2O, test 16 (○, 14.5 cm s^{-1} g.v.). Without CO_2 and H_2O, test 7 (Δ, 29.1 cm s^{-1} g.v.).

When only nitrogen, hydrogen and H_2S (2%) are used (test 7, Fig. 11), only water generated in reaction (1) will be present (approximately 2%). This is when the lowest H_2S values (Δ) are obtained in the outlet gases. Fig. 11 contains a comparison of tests 7, 10, 11 and 16. When 6% of CO_2 is introduced with no water (test 16) in such a way that the water present is that generated in reaction (1) plus that generated by reaction (7), there is more water (approximately 5.5%) and higher results are obtained than in the previous case but lower than when 10% of water is introduced, test no. 10 and test no. 11.

3.1.6. Conversion of calcium content in dolomite according to H_2S concentration in outlet gases and application to the case of 400 ppm of H_2S

Fig. 12 shows the curve of outlet H_2S normalised to 100% corresponding to test 12. (Table 2) (150 g dolomite, 14.5 cm s^{-1} gas velocity, 850 °C and grain size of 2–2.5 mm).

According to chemical analyses at the end of the test, CaO conversion to CaS was about 99%; therefore, the area over the curve in the plot represents the amount of H_2S used to convert practically all CaO into CaS (99%). This area can be calculated by integration of the amount adsorbed (20,000 ppm – H_2S content at each point) at each instant between 0 and the final time.

When integrating between 0 and each time point, the area represents the H_2S amount adsorbed up to that time. If this is ex-

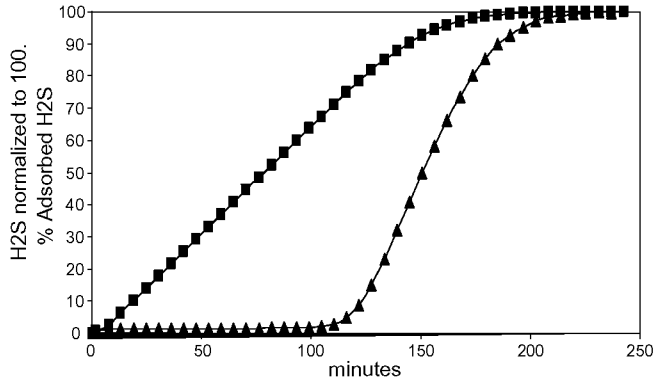

Fig. 12. Conversion to CaS during sulphurisation. H_2S breakthrough curve for test (Table 2) 12 (▲, 850 °C, 17 cm, 14.5 cm s^{-1}) and curve of% CaS conversion (■).

pressed as a percentage of total area, then the percentage of H_2S absorbed with respect to the total is obtained; this is equivalent to a conversion percentage of disposable CaO at the time considered and at the respective outlet H_2S concentration. When integrating at all time points corresponding to the points of the curve, the curve that represents the percentage of CaO conversion is obtained (■). As a result, this curve is also equivalent to the percentage conversion of Ca into CaS.

As observed initially, there is a practically linear growth that later tends towards a total of 100%.

For any particular outlet H_2S concentration, the time can be determined from the H_2S breakthrough curve. This time allows the percentage of calcium conversion to be determined from the other curve.

Table 3 shows the Ca conversion for tests carried out with samples of 2–2.5 mm for a concentration of 400 ppm of H_2S in the outlet gases.

Furthermore, under these conditions the concentration in the outlet gases is about 5 ppm of COS (see Section 3.2).

Table 3 shows how the percentage of calcium converted increases as gas velocity decreases (test 11 as compared with test 10), bed length increases (test 12 as compared with test 11, test 14 as compared with test 13, and test 18 as compared with test 17), initial H_2S decreases (test 17 as compared with test 10 and test 18 as compared with test 12) and steam concentration in the initial gas decreases (test 16 as compared with test 11).

3.2. Behaviour of COS

A total of 176 ppm of COS was introduced with the mixture of 2% H_2S.

When a silica bed was used (test 19) in the same way as dolomite at 850 °C and the gas contains only 2% H_2S, 18% H_2 and 176 ppm of COS (balanced to 100% with CO_2-free and steam-free N_2) and the same conditions are used as in a dolomite sulphurisation test, then the COS value at the outlet drops to approximately 1.5 ppm (already borderline for precision measurements using a gas chromatograph). Similarly, the H_2S content increases by approximately the same amount of COS, considering the relative errors to detect 176 ppm in 20,000. This shows that the following reaction is occurring:

$$COS + H_2 \leftrightarrow H_2S + CO \quad \Delta H^0 : +7.4\ \text{kJ mol}^{-1} \tag{9}$$

A similar reaction occurs when dolomite is sulphurised with the mixture of H_2S, H_2 and N_2 without adding CO_2 or water (as in test 7). Fig. 13 contains the results (Δ) of this test, which shows even when the sample is totally sulphurised, the outlet COS concentration is also practically 1.5 ppm (other curves under other conditions are shown in this figure).

Table 3
% Calcium converted to CaS at 400 ppm H_2S in the outlet gas (2–2.5 mm grain size, bottom position)

Test	Ca converted to CaS%	Test conditions			Inlet gas (N_2 balance gas)			
		Bed height (cm)	Gas velocity (cm s^{-1})	Temp (K)	H_2S%	H_2%	CO_2%	H_2O%
10	39	11.4	29.1	1123	2	18	6	10
11	49	11.4	14.5	1123	2	18	6	10
12	66	17	14.5	1123	2	18	6	10
13	40	11.4	14.5	1173	2	18	6	10
14	63	17	14.5	1173	2	18	6	10
16	58	11.4	14.5	1123	2	18	6	–
17	52	11.4	29.1	1123	0.4	19.6	6	10
18	74	17	14.5	1123	0.4	19.6	6	10

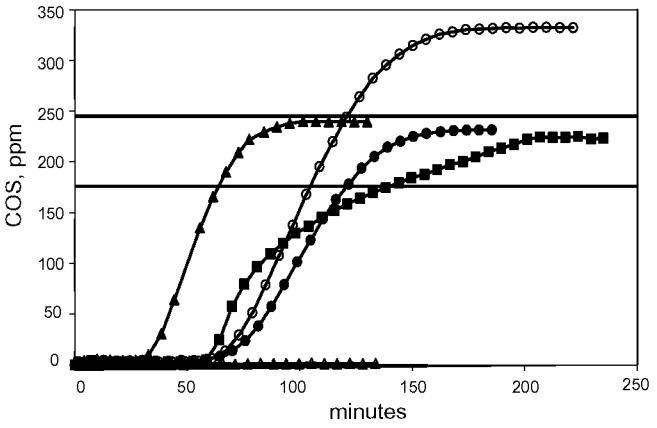

Fig. 13. COS in the outlet gas (11.4 cm). COS breakthrough curves with the usual inlet gas composition (2% H_2S, 6% CO_2, 10% H_2O) for tests (Table 2) 3 (■), 10 (▲), and 13 (●) and 20 (upper horizontal solid line) when silica is used instead dolomite. Without CO_2, test 16 (○). Without CO_2 and H_2O, test 7 (Δ). Lower horizontal solid line: COS introduced.

When silica is used (test 20, Table 2) and a mixture of 6% CO_2, 18% H_2, 10% H_2O and 2% H_2S (balanced to 100% with N_2) at 850 °C is passed, as used for most sulphurisation tests, the COS content of outlet gases becomes 245 ppm, in other words an increase in COS content is observed and a similar decrease in H_2S content is detected. This fact can be explained by reaction (9) due to increasing CO content as a result of the reverse water-shift reaction (7).

When dolomite is used under the same gas composition conditions, Fig. 14 (tests 3, 12 and 16), the COS and H_2S breakthrough curves have the same shape and are virtually identification, regardless of whether the curve is more or less "perfect". (To be able to compare both, the maximum amount produced by both composites is normalised to 100%.) The same occurs with the curve obtained with another different composition of sulphurant gas without added water (test 16) (● and ○).

This suggests that H_2S and COS are linked by one o more chemical equilibria and that there may be competition between reactions (3), (5), and (9). However, given the direct relationship of curve shape and the H_2S content with COS in each specific case of each curve, it seems that reactions (5) and (9) are the two that basically control the appearance of COS (the amount of CO_2 and H_2 present is much higher than the COS generated in all cases, except when neither CO_2 nor H_2O is used).

Under test conditions, the presence of CS_2 has not been detected in the outlet gases and, therefore, reaction (6) does not

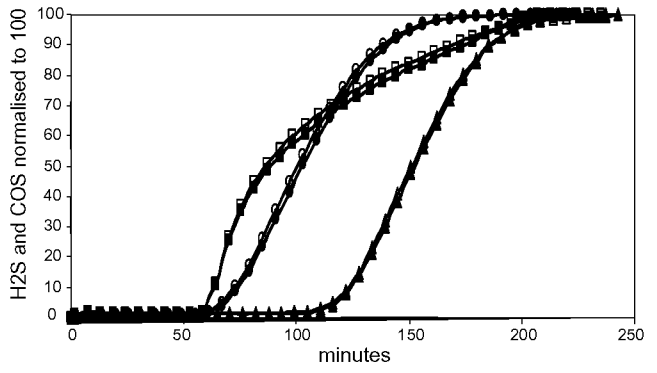

Fig. 14. H_2S and COS breakthrough curves under different operating conditions for tests (Table 2) 3 (■, □), 12 (▲, Δ) and 16 (●, ○). (H_2S: ■, ●, ▲, and COS: □, ○, Δ).

seem to take place in a detectable way. Under the gas chromatograph conditions used to analyse the outlet gases, the limit of graphical visual detection of the chromatographic pick of gases are about 1 ppm. As a result, another gas chromatograph detector, a differential mobility detector (DMD) specifically for sulphur compounds with a lower limit detection (under 0.1 ppm) was used; however, no signs of this compound were found.

Fig. 13 also shows the COS emission curves as absolute values of a series of tests carried out under different conditions (grain size, gas velocity) (tests 3, 10 and 13) but with the same gas composition (2% H_2S, 18% H_2, 6% CO_2 and 10% H_2O). Two lines have also been marked: one at 176 ppm corresponding to the amount introduced in the case of tests with 2% H_2S and another at 245 ppm corresponding to the amount present when the same gas is passed through silica at 850 °C (test 20, Table 2), which corresponds to the conditions of most tests carried out.

The curve corresponding to test 10 carried out under the same conditions as with silica gives a maximum COS value (▲) only slightly below that corresponding to silica, which demonstrates similar behaviour when dolomite is saturated or completely sulphurised. The curve corresponding to test 13 (●), carried out at a slower gas velocity and higher temperature (900 °C) shows a similar trend, although its peak value is slightly below the previous case. This also occurs with the curve from test 3 (■). In all cases, the value is higher than the initial COS content. This demonstrates the low influence of grain size, gas velocity and temperature (in the range of 850–900 °C tested) on maximum COS content if the gas composition is the same. This can be related to the equilibrium of chemical reaction (9) described above.

The influence of gas composition is evident in the curve from test 7 (Δ), carried out without added CO_2 or H_2O. This curve has been discussed above and shows emissions of about 1.5 ppm of COS. The behaviour is the same as for silica under the same conditions. This is easily explained by the equilibrium between H_2S and COS: if there is no CO except for the minimum amount produced by reaction (9), then this reaction is nearly completely shifted toward the right, causing the decomposition of COS.

In contrast with the above paragraph, test 16 (Table 2) done without added steam shows that higher values of COS were obtained. The main difference from the test is the non-addition of water: only water generated in reactions (1) and (7) is present (approximately 5.5%), leading to a higher level of CO. The curve shape is identical to that of H_2S (Fig. 13); however, because there is a higher absolute value than with the most frequent gas composition used, hydrolysis reaction (3) is reduced due to the lower presence of H_2O and the higher level of CO shifts reaction (9) toward the left contributing to this higher COS result.

3.3. *Influence on reverse water-shift reaction*

At the beginning of the sulphidisation process, when practically all H_2S reacts with CaO generated during dolomite calcination, an additional 2% of water is produced as in reaction (1) and this alters the equilibrium of reaction (7).

A variation in CO_2 is observed from start to finish of the sulphidisation process, in which practically no water is produced and in which only water introduced in the gaseous mixture takes part. Fig. 15 (test 12) shows that, in comparison with silica, the reaction rate is highly accelerated; the CO_2 level reached when dolomite is switched to silica is shown (solid line at the top of the plot).

The mean value calculated for the equilibrium constant of reaction (7) (eliminating the two initial points which are clearly outliers) is 1.14, a figure consistent with the theoretical value of this constant at 850 °C (1.144). The same occurs when operating at 900 °C or 950 °C.

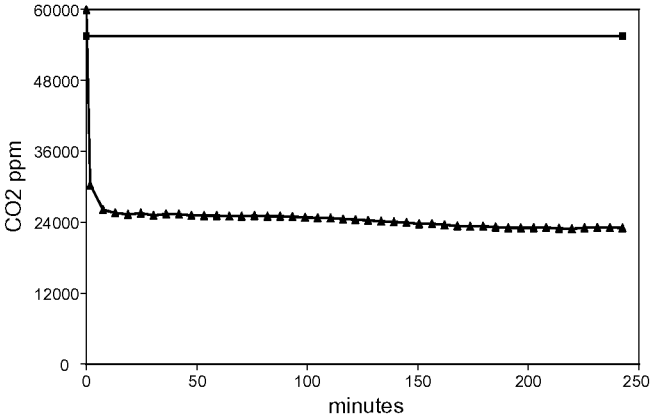

Fig. 15. Influence on reverse water-shift reaction. CO_2 curve for test (Table 2) 12 (▲, 850 °C, 17 cm, 14.5 cm s^{-1}) and test 20 (■, same conditions with silica instead calcined dolomite).

4. Conclusions

(1) The principal factors for the decrease in H_2S content in the outlet gases of the desulphuration column in the initial stages of bed use are gas velocity, bed length and inlet H_2S concentration. Lower gas velocities, lower inlet H_2S concentrations and higher bed lengths result in lower H_2S content in outlet gases.

(2) Dolomite position at the top of the desulphurant bed or bottom (under more static pressure) is another important factor that conditions its use. The behaviour at the bottom is worse with smaller grain sizes.

(3) A temperature between 850 °C and 950 °C has very little influence on the overall characteristics of the breakthrough curves and only a slight influence on the initiation of the curves due to the influence of temperature on the equilibrium constant.

(4) Lower steam and CO_2 concentrations in the inlet gas lead to significant reductions in the amount of H_2S present in the outlet gas in the initial adsorption stage of H_2S.

(5) To reach an upper threshold (e.g., 400 ppm) of H_2S at the outlet, dolomite conversion with a bed length of 17 cm is approximately 68% with 2% H_2S, 6% CO_2, 18% H_2 and 10% steam at the inlet and approximately 2.6% CO_2, 14.6% H_2 and 15.4% water at the outlet.

(6) Any COS present shows the same trend as H_2S in its breakthrough curves.

(7) Temperature (850 °C or 900 °C) has very little influence on the resulting COS.

(8) The amount of COS present in the outlet gases is highly dependent on the composition of the gas, especially the content of H_2S, H_2, CO and steam.

(9) Sulphidised dolomite acts as a catalyst for the reverse water-shift reaction, enhancing equilibrium at the temperature indicated. This should be considered when the intention is to produce hydrogen in the presence of CO_2.

Acknowledgements

The authors would like to thank the European Commission – DG Research, Research Fund for Coal and Steel (RFC-CR-04006) for supporting this study.

The authors would also like to thank UPM-R05/11205(RFC M0500204145) and UPM-CCG06-UPM/TQ-351 (RFC M0700204-178) for supporting this line of investigation of the research group.

Reference

Westmoreland PR, Gibson JB, Harrison DP. Comparative kinetics of high temperature reaction between hydrogen sulphide and selected metal oxides. Environ Sci Technol 1997;11:488–91.

Christoforu SC, Efthiniadis EA, Vasolos I. Sulphidation of mixed metal oxides in a fluidized bed reactor. Ind Eng Chem Res 1995;34:83–93.

Tomás-Alonso F, Palacios JM. Synthesis and surface properties of zinc ferrite spices in supported sorbents for hot-coal gas desulfurization. Fuel Process Technol 2004;80:191–203.

Pineda M, Palacios JM, Alonso L, García E, Moliner R. Performance of Zn oxide based sorbents for hot-coal gas desulfurization. Fuel 2000;79:885–95.

Alonso L, Palacios JM, Moliner R. The performance of some Zn based regenerable sorbents in hot coal gas desulphurization long-term using graphite as a pore-modifier additive. Energy Fuels 2001;15:1396–402.

Ahmed MA, Alonso L, Palacios JM, Cilleruelo C, Abanades JC. Structural changes in Zn ferrites as regenerable sorbents for hot coal gas desulphurization. Solid State Ion 2000;138:51–62.

Alonso L, Palacios JM, García E, Moliner R. Characterization of Mn and Cu oxides as regenerable sorbents for hot coal gas desulphurization. Fuel Process Technol 2000;62:31–44.

García E, Palacios JM, Alonso L, Moliner R. Performance of Mn and Cu mixed oxides as regenerable sorbents for hot coal gas desulfurization. Energy Fuels 2000;14:1296–303.

Alonso L, Palacios JM. Performance and recovering of a Zn-doped Mn oxide as a regenerable sorbent for hot-coal gas desulfurization. Energy Fuels 2002;16:1550–6.

Pan YG, Perales JF, Velo E, Puigjaner L. Kinetic behaviour of iron oxide sorbent in hot gas desulphurization. Fuel 2005;84:1105–9.

Risnes H, Fjellerup J, Henriksen H, Moilanen A, Norby P, Papadakis K, et al. Calcium addition in straw gasification. Fuel 2003;82:641–51.

Lin S, Harada M, Suzuki Y, Hatano H. Continuous experiment regarding hydrogen production by coal/CaO reaction with steam (I) gas products. Fuel 2004;83:869–74.

Adánez J, Diego LF, García-Labiano F, Abad A. Kinetics of H_2S reaction with calcined calcium-based sorbents. Energy Fuels 1998;12:617–25.

García-Labiano F, Adánez J, Abad A, Diego LF, Gayan P. Effect of pressure on the sulfidation of calcined calcium based sorbents. Energy Fuels 2004;18:761–9.

Adánez J, Abad A, Diego LF, García-Labiano F, Gayan P. Direct sulphidation of half-calcined dolomite under pressurized conditions. Ind Eng Chem Res 2004;43:4132–9.

Diego LF, García-Labiano F, Adánez J, Palacios JM. Factors affecting the H_2S reaction with non-calcined limestones and half-calcined dolomite. Energy Fuels 1999;13:146–53.

Abad A, Adánez J, García-Labiano F, Gayan P. Hot coal-gas desulphurization with calcium based sorbents in a pressurized moving-bed reactor. Energy Fuels 2004;18:1543–54.

Diego LT, Abad A, García-Labiano F, Adanez J, Gayán P. Simultaneous calcinations and sulfidation of calcium-based sorbents. Ind Eng Chem Res 2004;43:3261–9.

Adánez J, Abad A, García-Labiano F, Diego LF, Gayan P. H_2S retention with Ca-based sorbents in a pressurized fixed-bed reactor: application to moving-bed design. Fuel 2005;84:533–42.

Méndez-Vigo I, Elcogas. Puertollano IGCC update. In: Proceedings of gasification technologies international conference. San Francisco, USA <www.coal-ucg.com/publications2.html>; October 2002.

Yiqun Zhang, Zhongbin Xiao, Jianxin Ma. Hydrolysis of carbonyl sulphide over rare earth oxysulfides. Appl Catal B: Environ 2004;48:57–63.

Heesink ABM, Van Swaaij WPM. The sulphidation of calcined limestone with hydrogen sulphide and carbonyl sulphide. Chem Eng Sci 1995;50:2983–96.

Ishida Y, Taki U, Oyama H, Kitagawa K, Matsumoto K. Discriminative determination of hydrogen gas formed from tandem CO_2 reforming and shift reaction by isotope labelling followed by cryogenic gas chromatography. Fuel 2006;85:2041–5.

No-Kuk Park, Jong Bae Lee, Tae Jin Lee, Si Ok Ryu, Chih Hung Chang. The preparation of a high surface area metal oxide prepared by a matrix-assisted method hot gas desulphurization. Fuel 2005;84:2165–71.